Research Article | Vol. 26, No. 26 | 24 Dec 2018 | OPTICS EXPRESS 33764
Optics EXPRESS

Intense radioluminescence of NO/N_2-mixture in solar blind spectral region

THOMAS KERST[1,2,*] AND JUHA TOIVONEN[1]

[1]*Laboratory of Photonics, Tampere University of Technology, P.O. Box 692 33101 Tampere, Finland*
[2]*Helsinki Institute of Physics, Helsinki University, P.O. Box 64 00014 Helsinki, Finland*
[*]*thomas.kerst@tut.fi*

Abstract: Luminescence in air induced by alpha particle emitters can be used to optically detect radioactive contamination from distances that surpass the range of the alpha radiation itself. Alpha particles excite nitrogen molecules in air and the relaxation creates a faint light emission. When the composition of the gases surrounding the alpha particle emitter is altered then the luminescence spectrum changes. In this work, we report the creation of an intense light emission in the wavelength regime below 300 nm originating from alpha particle excited nitric oxide (NO). The light yield has been investigated as a function of the NO concentration in an N_2 atmosphere. Unlike the emission from molecular nitrogen, NO emits at wavelengths shorter than 300 nm, where solar background and artificial lighting are negligible, thus enabling optical detection of alpha radiation even under bright lighting conditions. We show that the radioactively induced NO emission reaches its maximum intensity at a concentration of 50 ppm of NO diluted in N_2. At this concentration, the strongest emission line of NO is about 25 times more intense than the most intense line of N_2 radioluminescence. Lastly, we discuss potential applications and limitations of the technique.

1. Introduction

Radioluminescence light is created when molecules excited by ionizing radiation relax radiatively to lower energy states and emit photons. The molecular excitations are caused mainly by numerous ionizing radiation induced secondary electrons, while they collide with the surrounding gas molecules [1]. The excited molecules relax either by non-radiative inelastic collisions with other molecules or by spontaneous radiative decay. The photon emitted in the latter process is said to be radioluminescent light and is indicative of the presence of ionizing radiation. Alpha radiation causes the most localized radioluminescence source as alpha particles lose their energy in about 4 cm in air, whereas beta and gamma radiation ionize air in the range of about 1 m and 50 m, respectively. The range of the induced light greatly surpasses the range of the alpha particles themselves, making alpha induced radioluminescence well suited for remote detection of radioactive sources [2].

The radioluminescence in air is generated mostly by emission of molecular nitrogen. The most intense N_2 emission lines are generated when a N_2 molecule radiatively decays from the $C^3\Pi_u$ state to an energetically lower $B^3\Pi_g$ state, and thereby emits an ultraviolet (UV) photon. Similarly, ionized nitrogen N_2^+ emits at the same wavelength band. Together, the N_2 molecules and ions compose narrow emission lines in the spectral range from 280 nm to 430 nm [3]. Also other molecules in air can produce a faint radioluminescence. However, the emission of nitrogen is utilized in all the recent applications that aim to detect alpha radiation from a distance [2,4–7].

Molecular nitrogen that surrounds an alpha emitter is effectively turned into a light source that emits on UV wavelengths. The spectrum of this light source is indicative of the presence of a nearby radioactive source, and for locating the source, it is thus sufficient to detect the origin of the UV light at the area under investigation. A single alpha particle causes the generation of about 100 UV photons in normal air and about 600 UV photons in a nitrogen

#344807 https://doi.org/10.1364/OE.26.033764
Journal © 2018 Received 31 Aug 2018; revised 15 Nov 2018; accepted 18 Nov 2018; published 12 Dec 2018

Optics EXPRESS

atmosphere [8]. As a consequence, even a strong alpha emitter generates a light emission that is much weaker than the light emission from light bulbs or even dimly-lit exit signs. An obvious way to overcome this obstacle is to filter the measured light and discriminate the UV light from visible light. Wavelengths of light that are associated with nitrogen emission are transmitted while everything else is rejected. This approach works well for environments in which no UV light from other sources than the radioluminescence is present [3,9,10].

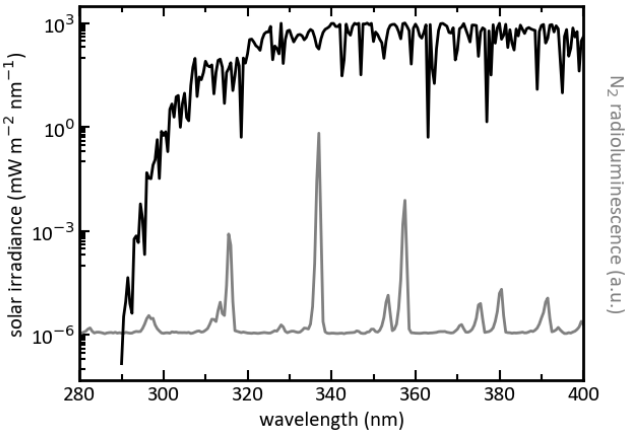

Fig. 1. Spectrum of sunlight reaching the earth's surface (black) contrasted with the radioluminescence of N_2 (gray) in the wavelength range 280 nm – 400 nm. The solar irradiance (AM1.5 Global tilt [11]) is displayed on a logarithmic scale, while the N_2 emissions are shown on a linear scale. At wavelengths longer than 290 nm the solar irradiance spectrally overlaps with the radioluminescence of N_2.

The spectral filtering is of limited use in normal lighting conditions. The spectrum of sunlight reaching the earth contains UV components that overlap with the nitrogen radioluminescence spectrum, and similarly, the most of typical artificial lighting solutions contain UV wavelengths. Consequently, the radioluminescence cannot be discriminated from the background lighting. Figure 1 shows the spectrum of the solar radiation reaching the earth's surface together with the nitrogen emission spectrum. It can be seen that the solar irradiance for wavelengths shorter than 300 nm is drastically diminished, which is due to the absorption of these wavelengths in the atmosphere by ozone [12]. This is region is called a solar blind (SB) spectral region, which is so deep in the UV that it is free of artificial lighting, too, and optical measurements can be conducted without an interference from the lighting conditions. A small fraction of the nitrogen emission is at the wavelengths shorter than 290 nm. Thus, standoff detection of alpha radiation is possible even under bright lighting by measuring this small fraction of the radioluminescence with solar blind UV photodetection [7].

A different approach to overcome the problem with interfering background lighting is to utilize the luminescence of molecules other than nitrogen. Nitric oxide (NO) is known to emit light in the solar blind spectral region. This light originates from a radiative transition from the $A^2\Sigma^+$ state to the ground state $X^2\Pi$ of NO emitting a photon with a wavelength between 220 nm and 305 nm. The spectrum formed by this emission is called the NO γ-band [13]. The intensity of the NO emission is critically dependent on the content of the surrounding gas, as many colliding molecules are capable of quenching the excited state, thereby eliminating its possibility for the radiative transition. Even in small amounts, molecular oxygen causes most of the NO excitations to decay without emitting a UV photon.

In this work, we present a spectrum of nitric oxide radioluminescence and show that its intensity can exceed that of nitrogen. We investigate the intensity of the NO radioluminescence as a function of the NO concentration in an N_2 atmosphere and show that

Optics EXPRESS

the most intense radioluminescence is achieved at a concentration of about 50 ppm. The radioluminescence spectrum of the NO/N_2-mixture is recorded at the wavelength range from 200 nm to 400 nm. It shows that the strong NO radioluminescence is indeed in the solar blind spectral region. With this approach, we overcome two major limitations of the standoff detection of alpha radiation conducted under normal lighting conditions. First, the radioluminescence signal is free from interference caused by the background lighting. Second, under proper conditions, nitric oxide radioluminescence photons are substantially more numerous than those of nitrogen radioluminescence. Under ideal conditions, the strongest NO peak is about 25 more intense the strongest N_2 radioluminescence peak. Compared to the amount of photons generated from N_2 radioluminescence is normal air, the NO radioluminescence is about 150 times more intense. This can be utilized to either lower the detection limit or for remote detection from larger distances.

2. Experiments and methods

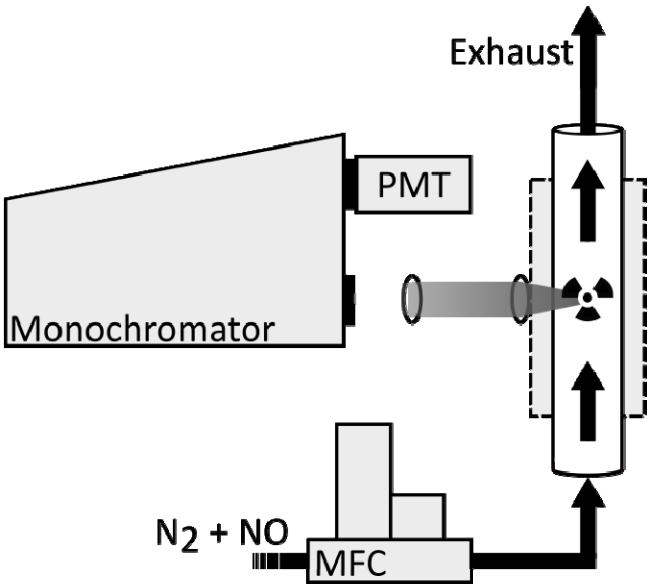

Fig. 2. Schematic illustration of the experimental setup. An alpha radiating source is located within a flow tube made of quartz glass. The tube is constantly flushed with a mixture of N_2 and NO. A monochromator and a PMT are used to record the radioluminescence intensity at a specified wavelength.

Figure 2 shows a schematic illustration of the experimental setup used in this work. All measurements were carried out by placing a 32 MBq alpha active AM-241 source in a 25-mm-diameter quartz tube (Robson scientific). A 21-mm-thick steel mantle, protecting personnel and equipment from gamma radiation of the source, surrounded the parts of the tube close to source. A cone shaped hole with the f-number f/1.378 in the steel mantle allowed light originating in the quartz tube to escape. The light was guided via a Keplerian telescope (Thorlabs LA4052-UV, 35 mm and LA4924-UV, 175 mm) to a computer controlled monochromator (Horiba iHR 550). The telescope was matched to both f-numbers of the steel mantle opening and the monochromator entrance to guarantee optimal light collection efficiency. The monochromator selected a wavelength and guided it to a photon counting photomultiplier tube (PMT, Perkin-Elmer MP-1082). The monochromator was operated with slits of 0.5 mm in width resulting a spectral resolution of 0.45 nm. The gas in the quartz tube was controlled with two mass flow controllers (Bronkhorst High-Tech, 18BRF-201CV-1K0 and 18BRF-201CV-20K). The first controller was attached to a gas bottle filled with 1500 ppm of NO in type 5.0 N_2 (AGA). The latter one was connected to a

Optics EXPRESS

bottle filled with type 6.0 N_2 (AGA). The end of the quartz tube not attached to the controllers was connected to an exhaust. All tubing was kept as short as possible to prevent the formation of large dead volumes.

The intensity of the γ-band emission as a function of the NO concentration in N_2 was measured by constantly flushing the tube with 3 SLPM of a mix consisting of N_2 and varying the concentration of NO. The concentration of the mixture was controlled with the mass flow controllers. The NO concentration was increased in 2 min intervals, starting from 25 ppm and ranging to 300 ppm with a total of 18 different concentrations. After each change in concentration, we waited for 60 s to let the gas mixture become a homogeneous mix. Then we recorded the photons with an associated wavelength of 236 nm travelling through the monochromator with the PMT using an integration time of 60 s.

The radioluminescence spectrum was recorded by scanning the monochromator in 0.5 nm steps from 200 nm to 400 nm. At each step, the number of photons reaching the PMT was recorded for a total of 60 s. During the entire spectrum scan, the atmosphere inside the glass tube consisted of 50 ppm of NO dissolved in N_2.

3. Results and discussion

The radioluminescence intensity of NO was recorded at 236 nm as a function of the NO concentration in constantly flowing N_2 carrier gas. Figure 3 shows the intensity of the radioluminescence as counts per second of the recording photon counting PMT detector. Recording of the intensity only at one of the NO lines at 236 nm is considered well representative measurement for the relative NO radioluminescence intensity as all the NO emission lines originates from the same γ-band transition. It can be seen that the NO radioluminescence intensity increases with the increasing NO concentration. This holds true up to a concentration of 50 ppm, after which the intensity decreases.

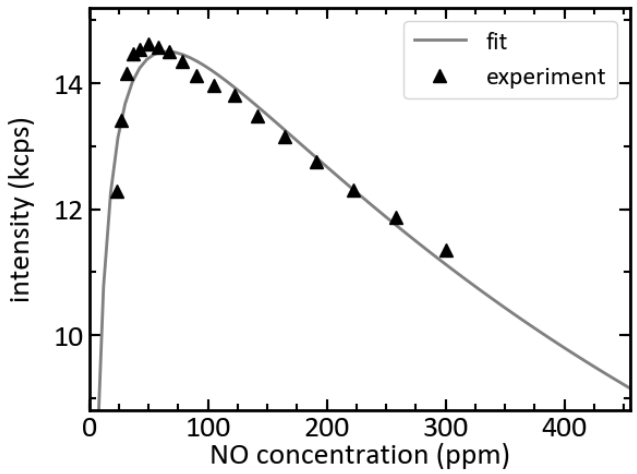

Fig. 3. Intensity of NO emissions recorded at 236 nm as a function of the NO concentration in an N_2 atmosphere. The intensity is recorded with a photon counting PMT and presented in thousands of counts per seconds (kcps). The concentration sweep has been made from low to high NO concentrations. The maximum in the intensity is reached at the NO concentration of about 50 ppm. The gray line, based on Eqs. (1), (2) and (3) is a fit to the data having a coefficient of determination of $R^2 = 0.93$.

The recorded curve suggests that the mechanism by which the nitric oxide radioluminescence is produced is different than that of N_2 radioluminescence. When N_2 radioluminescence is created, the nitrogen gets electronically excited mainly due to free electrons created by the alpha particle. The radiative decay of this excitation then gives rise to radioluminescence. If a similar direct excitation would be assumed to be the cause for NO

Optics EXPRESS

radioluminescence, then the shape of the curve showing the radioluminescence intensity as a function of the NO in concentration would be a linear increase until affected by NO self-quenching. Using the quenching coefficients from Settersten et al. [14] this point of maximum concentration can be estimated to be about 5000 ppm. This is in contrast to our observation and we can therefore conclude that the radioluminescence mechanism in the case of the NO/ N_2- mixture is different from the one observed with nitrogen radioluminescence.

Excitation of NO by excitation transfer via interaction with N_2 molecules appears to be able to explain our data. In this process, molecular nitrogen in the long-lived N_2 $A^3\Sigma_u^+$ state excites ground state nitric oxide to the NO $A^2\Sigma^+$ state, while the N_2 molecule loses its excitation and decays to the ground state [21]. If this excitation mechanism is assumed to be the predominant excitation mechanism of NO, then the dynamics of the system can be described by the following rate equations

$$\frac{\mathrm{d}}{\mathrm{d}t}c_{\mathrm{N}_2^X} = \alpha c_{\mathrm{N}_2^X} - \frac{c_{\mathrm{N}_2^A}}{\tau_{\mathrm{N}_2}} - k_{et}c_{\mathrm{N}_2^A}c_{\mathrm{NO}^X} \tag{1}$$

$$\frac{\mathrm{d}}{\mathrm{d}t}c_{\mathrm{NO}^A} = k_{et}c_{\mathrm{N}_2^A}c_{\mathrm{NO}^X} - \frac{c_{\mathrm{NO}^A}}{\tau_{\mathrm{NO}}} - q_{\mathrm{N}_2}pc_{\mathrm{NO}^A}c_{\mathrm{N}_2^X} - q_{\mathrm{NO}}pc_{\mathrm{NO}^A}c_{\mathrm{NO}^X}, \tag{2}$$

where $c_{\mathrm{N}_2^X}$ / $c_{\mathrm{N}_2^A}$ is the concentration of nitrogen in the excited state / ground state. The sum of both number concentration is assumed to be constant at all times. Likewise, c_{NO^X} / c_{NO^A} is the concentration of nitric oxide in the exited state / ground state. Further, we assume that the gas is only made up of these four components, thus the sum of all four concentrations equals to 1. τ_{N_2} and τ_{NO} are the radiative lifetimes of the excited state of molecular nitrogen and nitric oxide, respectively. q_{N_2} and q_{NO} are the quenching coefficients describing the quenching of excited NO by the presence of ground state nitrogen and ground state nitric oxide, respectively. We do not take into consideration the quenching effects by other molecules, since ground state nitrogen and nitric oxide ideally make up the entire gas mixture. p = 760 Torr is the pressure of the gas. α describes the excitation of ground state N_2 by the presence of the radioactive source. We assume α to be a small value larger than 0. As long as α is not too large, it's numerical value hardly matters, since it does not influence the dynamics of the system but solely determines the magnitude of the observed radioluminescence. k_{et} is the excitation transfer rate and in our model the only mechanism effectively populating the excited state of NO.

We retrieve the values for $c_{\mathrm{N}_2^A}$ and c_{NO^A} from Eqs. (1) and (2) for a given concentration of nitric oxide using numerical evaluation. The system is assumed to be in equilibrium at the time of measurement, which allows us to set the both Eqs. (1) and (2) to 0. We solve them numerically by computing the eigenvalues of the associated matrices using the linear algebra package NumPy with Python 3.6. The eigenvalue problem has to be solved separately for each nitric oxide concentrations. This gives us the equilibrium concentration of NO in excited state c_{NO^A} as a function of k_{et} and the ground state NO concentration in the system c_{NO^X}. We still need to evaluate how many photons these excited states of NO emit, before fitting to the recorded radioluminescence curve in Fig. 3 can be made.

Solving the number of NO emitted photons per unit of time requires evaluation of the excited nitric oxide fraction that decays radiatively, i.e. the quantum efficiency QE for the luminescence. The QE can be evaluated by comparing the radiative decay rate to the sum of all possible decay rates from Eq. (2), resulting in

Optics EXPRESS

$$\mathrm{QE} = \frac{c_{\mathrm{NO}}\tau_{\mathrm{NO}}^{-1}}{c_{\mathrm{NO}}\tau_{\mathrm{NO}}^{-1} + q_{\mathrm{N_2}}\, p c_{\mathrm{NO}^A} c_{\mathrm{N_2}^X} + q_{\mathrm{NO}}\, p c_{\mathrm{NO}^A} c_{\mathrm{NO}^X}}, \tag{3}$$

where the denominator term includes the radiative decay, nitrogen quenching and nitric oxide self-quenching. The total number of photons reaching the detector per unit of time is found by weighing the concentration of excited nitric oxide with the quantum efficiency. This number is multiplied with a free scaling constant C accounting for the alpha activity and for the geometry of our detection scheme, yielding to total number of detected photons

$$\Phi = C \cdot \mathrm{QE} \cdot c_{\mathrm{NO}^A} = \frac{c_{\mathrm{NO}^A}}{1 + \tau_{\mathrm{NO}}\, p \left(q_{\mathrm{N_2}} c_{\mathrm{N_2}^X} + q_{\mathrm{NO}} c_{\mathrm{NO}^X} \right)}. \tag{4}$$

The number of photons detected as a function of the nitric oxide concentration c_{NO^X} is mainly determined by the excitation transfer rate k_{et}, affecting c_{NO^A}, and the nitric oxide self-quenching rate q_{NO}. Therefore, we treated them, along with the scaling constant C, as free parameters in the fitting, while assigning fixed values to all other parameters from literature [3,14,15].

The solution fits the data with a coefficient of determination $R^2 = 0.93$. Our fitted value for k_{et} is 63 kHz. This deviates by roughly 30% from the value of 89 kHz predicted by Piper et al. [16] for NO concentration of 50 ppm. Likewise, our fitted value is about 20% - 30% lower than other published values [17–19], which might relate to a slightly slower excitation transfer rate in our system or be a result of measurement uncertainty of the experimental setup. The fitted value for q_{NO} is $8.5 \cdot 10^6$ Hz Torr^{-1}. This is within the predictions of $8.17 \cdot 10^6$ Hz Torr^{-1} by Settersten et al. [14], $8.9 \cdot 10^6$ Hz Torr^{-1} by Paul et al. [20], and $8.9 \cdot 10^6$ Hz Torr^{-1} by Tamura et al. [21] indicating that the decrease in radioluminescence intensity with an increasing concentration of NO is fully determined by the self-quenching. Overall, the model fits to our data very well, and we can conclude that the excitation transfer from nitrogen to nitric oxide does play a dominant role in the occurrence and characteristics of NO radioluminescence.

In Fig. 4 we present the radioluminescence spectrum of the NO/N_2-mixture having NO concentration of 50 ppm. The NO γ-band emission lines dominate the recorded radioluminescence spectrum at wavelengths between 200 nm and 300 nm. Radioluminescence of nitrogen lines at wavelengths longer than 300 nm remain about at the same intensity than with pure nitrogen atmosphere. Thus, the amount of total energy emitted as radioluminescence significantly increases in comparison to the gas atmosphere of air or pure nitrogen. In Table 1 we present a side-by-side comparison of the radioluminescence yield and the energy conversion efficiencies when an alpha particle is stopped in different gases. Our demonstrated 50 ppm of NO in N_2 generates a radioluminescence photon count rate that is 25 times larger than that of nitrogen radioluminescence, and thus about 150 times larger compared to the radioluminescence in air using values reported by Sand et al. [8]. In energy conversion efficiency from kinetic energy of an alpha particle to radioluminescence photon energy this yields to 200 times larger conversion efficiency in the NO/N_2-mixture than in air due the difference in emitted photon energies. The resulted energy conversion efficiency of 2% is already a remarkably large value enabling enhanced detection limits in optical detection of radiation.

Optics EXPRESS

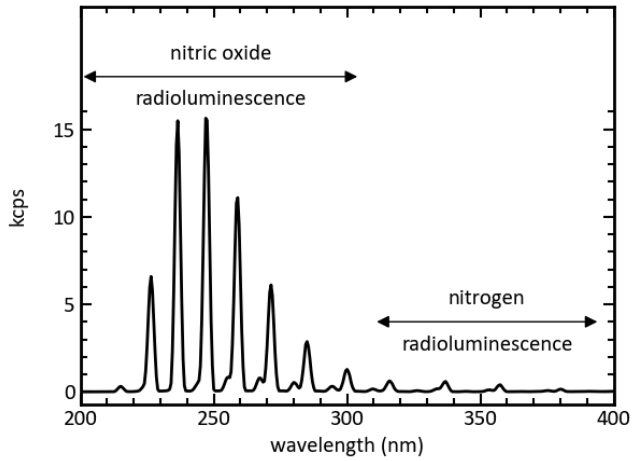

Fig. 4. Radioluminescence spectrum of gas a gas mixture containing 50 ppm of NO diluted in N_2. The nitric oxide emission is about 25 times stronger than N_2 emission and most of the NO emission lines are located in the solar blind spectral region.

Table 1. The intensity of radioluminescence between 200 nm – 400 nm for three different gas environments. The intensity is expressed in relation to the intensity found in normal air, highlighting the improvement in photon yield by changing gases. The energy conversion efficiency shows how much of the energy deposited in air by an alpha particle is emitted as light.

Gas environment	Radioluminescence intensity	Energy conversion Efficiency	Reference
Air	1	$1{\cdot}10^{-4}$	Ref. 8
Nitrogen	6	$6{\cdot}10^{-4}$	Ref. 8
50 ppm of NO/N_2	150	$2{\cdot}10^{-2}$	This work

Using nitric oxide radioluminescence is especially helpful when working under bright lighting conditions. NO emission spectrum does not overlap with sunlight or artificial lighting, thus enabling the use of background-free solar blind optical detection. A detection system being solar blind means that it is insensitive to light at wavelengths longer than 300 nm, while being sensitive to wavelengths shorter than 300 nm. Sand et al. [7] reported about a stand-off solar blind radioluminescence scanner that was able to map locations of alpha radiation sources at the distance of 1 m. The resulted limit of detection in air atmosphere was 800 kBq due to very low amount of nitrogen luminescence at the wavelengths shorter than 300 nm. That is too high activity level for many safety applications. However, radioactive materials are often handled in closed gloveboxes were the gas atmosphere can be controlled. In typical nitrogen atmosphere Sand et al. [7] achieved already more reasonable 6 kBq limit of detection that was attributed to minor NO impurities in the system. Comparing that with our results indicate that introducing 50 ppm of NO in the nitrogen atmosphere would enhance the limit of detection down to 16 Bq. That would be a remarkable enhancement in the performance and still possible to operate under normal lighting. However, introducing 50 ppm of NO is not viable in many cases due to safety and corrosion reasons. We estimated from our model that already 1 ppm trace amount of NO would increase the radioluminescence remarkably at the solar blind spectral region up to the level of pure nitrogen luminescence at longer wavelengths yielding about 400 Bq limit of detection in presented solar blind application by Sand et al. [7]. That is more than 10 times better performance than under nitrogen atmosphere and worth to consider in applications were the gas atmosphere can be controlled.

Optics EXPRESS

4. Conclusions

We presented the creation of intense radioluminescence in the solar blind spectral region using nitric oxide. By monitoring the NO radioluminescence intensity as a function of the amount of NO that is diluted in N_2 we demonstrated that the excitation mechanism for NO is different from that of N_2 radioluminescence. We showed that an excitation transfer from radiatively excited N_2 is the main mechanism for NO excitation, which yields to a maximum energy conversion efficiency of 2% from kinetic energy of alpha particle to optical photons at NO concentration of 50 ppm. At this concentration NO radioluminescence is 25 times more intense than that of pure nitrogen. Our results indicate that adding a trace amounts of nitric oxide into nitrogen atmosphere is a potential method for optical alpha radiation detection in under bright lighting conditions.

Funding

Business Finland, Finland Distinguished Professors (FiDiPro), Project: Novel Instrumentation for Nuclear Safety, Security and Safeguard (NINS3)

References

1. F. Arqueros, F. Blanco, and J. Rosado, "Analysis of the fluorescence emission from atmospheric nitrogen by electron excitation, and its application to fluorescence telescopses," New J. Phys. **11**(6), 065011 (2009).
2. S. M. Baschenko, "Remote optical detection of alpha particle sources," J. Radiol. Prot. **24**(1), 75–82 (2004).
3. A. Lofthus and P. H. Krupenie, "The spectrum of molecular nitrogen," J. Radiol. Prot. **24**(1), 75–82 (1977).
4. F. Lamadie, F. Delmas, C. Mahe, P. Gironès, C. Le Goaller, and J. R. Costes, "Remote alpha imaging in nuclear installations: new results and prospects," IEEE Trans. Nucl. Sci. **52**(6), 3035–3039 (2005).
5. J. Sand, S. Ihantola, K. Peräjärvi, A. Nicholl, E. Hrnecek, H. Toivonen, and J. Toivonen, "Imaging of alpha emitters in a field environment," Nucl Instrum. Meth. A **782**, 13–19 (2015).
6. D. S. Haslip, T. Cousins, V. Koslowsky, and H. Ing, H. R. Andrews, E. T. H. Clifford, and D. Locklin, "Standoff radiation imaging detector," U.S. patent US7317191B1 (8. Jan. 2008).
7. J. Sand, A. Nicholl, E. Hrnecek, H. Toivonen, J. Toivonen, and K. Peräjärvi, "Stand-off radioluminescence mapping of alpha emitters under bright lighting," IEEE Trans. Nucl. Sci. **63**(3), 1777–1783 (2016).
8. J. Sand, S. Ihantola, K. Peräjärvi, H. Toivonen, and J. Toivonen, "Radioluminescence yield of alpha particles in air," New J. Phys. **16**(5), 053022 (2014).
9. P. Colin, A. Chukanov, V. Grebenyuk, D. Naumov, P. Nédélec, Y. Nefedov, A. Onofre, S. Porokhovoi, B. Sabirov, and L. Tkatechev, "Measurement of air and nitrogen fluorescence light yields induced by electron beam for UHECR experiments," Astropart. Phys. **27**(5), 317–325 (2007).
10. J.-F. Pineau and G. Imbard, "Remote alpha source location device and method," US Patent 6281502B1 (2001).
11. National Renewable Energy Laboratory, "Direct and Global 37 Deg Tilt: ASTM G-173," *http://rredc.nrel.gov/solar/spectra/am1.5/ASTMG173.html*, Accessed 4 October 2017.
12. R. D. Hudson, "Critical review of ultraviolet photabsorption cross sections for molecules of astrophysical and aeronomic interest," Rev. Geophys. **9**(2), 305–406 (1971).
13. J. Danielak, U. Domin, R. Kepa, M. Rytel, and M. Zachwieja, "Reinvestigation of the emission gamma band (A2S+-X2P) system of the NO molecule," J. Mol. Spectrosc. **181**, 394–402 (1997).
14. T. B. Settersten, B. D. Patterson, and J. A. Gray, "Temperature- and species-dependent quenching of NO A 2Sigma+(v′=0) probed by two-photon laser-induced fluorescence using a picosecond laser," J. Chem. Phys. **124**(23), 234308 (2006).
15. A. B. Callear and M. J. Pilling, "Fluorescence of nitric oxide. Part7.—quenching rates of NO C 2 P (v=0), its rate of radiation to NO A 2 S+, energy transfer efficiencies, and mechanisms of predissociation," Trans. Faraday Soc. **66**(0), 1618–1634 (1970).
16. L. G. Piper, L. M. Cowles, and W. T. Rawlins, "Einstein coefficients and transition moment variation for the NO (A^2S+-X2P) transition," J. Chem. Phys. **85**, 3369–3378 (1986).
17. J. W. Dreyer, D. Perner, and C. R. Roy, "Rate constants for the quenching of N_2 ($A3Su^+$, va=0-8) by CO, CO_2, NH_3, NO, and O_2," J. Chem. Phys. **61**(8), 3164–3169 (1974).
18. W. G. Clark and D. W. Setser, "Energy transfer reactions of N2 (A3. SIGMA. u+). 5. Quenching by hydrogen haildes, methyl haildes, and other molecules," J. Phys. Chem.-US **84**(18), 2225–2233 (1980).
19. R. A. Young and G. A. St. John, "Experiments on N2(A3Su+). Ii. Excitation of NO," J. Chem. Phys. **48**(2), 898–900 (1968).
20. P. H. Paul, J. Gray, J. L. Durant, and J. W. Thomann, "Collisional quenching corrections for laser-induced fluorescence measurement of NO A2S+," AIAA J. **32**(8), 1670–1675 (1994).
21. M. Tamura, P. A. Berg, J. E. Harrington, J. Luque, J. B. Jeffries, G. P. Smith, and D. R. Crosley, "Collisional quenching of CH(A), OH(A), and NO(A) in low pressure hydrocarbon flames," Combust. Flame **114**(3), 502–514 (1998).